Exploiting Cell-Free Systems

Bujara, Matthias; Schümperli, Michael; Billerbeck, Sonja; Heinemann, Matthias; Panke, Sven

Published in:
Biotechnology and Bioengineering

DOI:
10.1002/bit.22666

Publication date:
2010

ARTICLE

BIOTECHNOLOGY and BIOENGINEERING

Exploiting Cell-Free Systems: Implementation and Debugging of a System of Biotransformations

Matthias Bujara,[1] Michael Schümperli,[1] Sonja Billerbeck,[1] Matthias Heinemann,[2] Sven Panke[1]

[1]Bioprocess Laboratory, Department of Biosystems Science and Engineering, ETH Zurich, Mattenstrasse 26, 4058 Basel, Switzerland; telephone: 41-61-387-32-09; fax: 41-61-387-39-94; e-mail: sven.panke@bsse.ethz.ch

[2]Institute of Molecular Systems Biology, ETH Zurich, Zurich, Switzerland

Received 18 September 2009; revision received 4 December 2009; accepted 7 December 2009

Published online 20 January 2010 in Wiley InterScience (www.interscience.wiley.com). DOI 10.1002/bit.22666

ABSTRACT: The orchestration of a multitude of enzyme catalysts allows cells to carry out complex and thermodynamically unfavorable chemical conversions. In an effort to recruit these advantages for in vitro biotransformations, we have assembled a 10-step catalytic system—a system of biotransformations (SBT)—for the synthesis of unnatural monosaccharides based on the versatile building block dihydroxyacetone phosphate (DHAP). To facilitate the assembly of such a network, we have insulated a production pathway from *Escherichia coli*'s central carbon metabolism. This pathway consists of the endogenous glycolysis without triose-phosphate isomerase to enable accumulation of DHAP and was completed with lactate dehydrogenase to regenerate NAD^+. It could be readily extended for the synthesis of unnatural sugar molecules, such as the unnatural monosaccharide phosphate 5,6,7-trideoxy-D-threo-heptulose-1-phosphate from DHAP and butanal. Insulation required in particular inactivation of the *amn* gene encoding the AMP nucleosidase, which otherwise led to glucose-independent DHAP production from adenosine phosphates. The work demonstrates that a sufficiently insulated in vitro multi-step enzymatic system can be readily assembled from central carbon metabolism pathways.

Biotechnol. Bioeng. 2010;106: 376–389.

KEYWORDS: cell-free synthesis; carbohydrate synthesis; multi-enzyme catalysis; dihydroxyacetone phosphate; aldolase

Introduction

Cell-free systems are a promising approach for the implementation of novel complex biochemical functions (Forster and Church, 2007; Jewett et al., 2008; Meyer et al., 2007). The absence of physical barriers such as membranes and their specific transportation mechanisms allows for direct substrate supply and access to the product and the catalytic system, enabling facilitated monitoring and manipulation, and the application of user-defined conditions (Hold and Panke, 2009).

The downsides of these advantages are typically a loss of catalytic complexity and the inability of the system to repair itself. However, the former issue can be successfully addressed by either in vitro re-assembling of multi-member systems from purified components or by using cell-free extracts (CFXs). Purified systems allow an unsurpassed degree of reaction control (e.g., Fessner and Walter, 1992; Nahalka et al., 2003; Shimizu et al., 2001; Welch and Scopes, 1985; Zhang et al., 2007), and have been successfully used in tasks as complex as in vitro protein production (Shimizu et al., 2001). The obvious drawback is currently the laborious purification of the parts. Reaction systems based on CFXs, which only remove the cellular transport barrier, have been exploited to similar degrees of complexities (Mureev et al., 2009; Swartz, 2006), but frequently suffer from undesired background reactions (Kim and Swartz, 2000, 2001), which in turn might be eliminated in selectively mutated strains (Calhoun and Swartz, 2006; Knapp et al., 2007).

The problem of undesired background reactions is exemplified in the central carbon metabolism of bacteria, which has a number of molecules as intermediates that could be of ample use in fine-chemical syntheses such as dihydroxyacetone phosphate (DHAP), phosphoenol pyruvate (PEP; Enders et al., 2008), pyruvate (PYR; Zelic et al., 2003) and erythrose-4-phosphate (E4P; Sheflyan et al., 1998), but at the same time is a highly interconnected reaction network with ample possibilities to interfere with designed reaction pathways. Of the various interesting targets, DHAP is central to the production of a stereochemically complete set of vicinal diols and its chemical or biochemical synthesis has therefore received a lot of

Correspondence to: S. Panke

attention (Herk et al., 2009; Schümperli et al., 2007). We therefore investigated whether glycolysis as a part of central carbon metabolism could be adapted for the in vitro production of DH AP from cheap glucose (GLC).

Material and Methods

Chemicals

NAD^+ and NADH were from Gerbu (Heidelberg, Germany), yeast extract and peptone from BD Bioscience (Basel, Switzerland), ATP and purified enzymes from Roche Diagnostics (Rotkreuz, Switzerland), except myokinase and rabbit muscle aldolase (RAMA; Sigma–Aldrich, Buchs, Switzerland). All other chemicals were from Sigma–Aldrich.

Strains and Growth Condition

Escherichia coli W3110 (ATCC 27325) and two derivatives, the knockout strains W3110 *tpiA::kan* and W3110 *tpiA::kan amn*, were used in this study. W3110 *tpiA::kan* was constructed by phage λ red recombination as described previously (Datsenko and Wanner, 2000). The *tpiA* gene was replaced by a kanamycin resistance gene (Datsenko and Wanner, 2000) flanked by 40 bp segments that were homologous to the *tpiA* gene using the upstream primer 5′-GTTAAGGCGAAGAGTTAAGGAAAGTAAGTGCCGGA-TATGA-3′ and the downstream primer 5′-CGTGGA-GAATTAAAATGCGACATCCTTTAGTGATG GGTAA-3′.

W3110 *tpiA::kan amn* was constructed by removing the kanamycin resistance gene from W3110 *tpiA::kan* and subsequent P1-transduction (Miller, 1992) of the *amn::kan* mutation from W3110 *amn::kan* (Baba et al., 2006). Knockouts were verified by PCR using appropriate primers. The strains were grown in Luria–Bertani broth. For fermentations M9-GYE (M9 mineral medium supplemented with 4 g L^{-1} GLC and 5 g L^{-1} yeast extract) was used. LB and M9 media were prepared as described elsewhere (Sambrook and Russel, 2001). Kanamycin was added to 50 μg mL^{-1}.

Fermentation and Preparation of CFX

Fermentations were carried out as fed-batch fermentations using M9-GYE medium. An overnight culture in the same medium plus kanamycin was used for inoculation of 3 L of medium in a 5 L bioreactor equipped as described earlier (Valsesia et al., 2007) to an initial OD_{600} of 0.5. The fermentation was started in batch mode and the feed (100 g L^{-1} yeast extract, 50 g L^{-1} GLC, 22.2 mM $MgSO_4$) was started after the culture had entered stationary phase (as indicated by a rise in the dissolved oxygen tension). The feeding rate was controlled manually such that the dissolved oxygen concentration never fell below 40% of saturation to prevent oxygen limitation. Aeration was set to 3 L min^{-1} (1 vvm) and stirrer speed to 800 rpm during batch phase. They were increased during the feed-phase to 1,000 rpm and 5 L min^{-1} to increase oxygen transfer. Fermentations were stopped at an OD_{600} of 18–20 corresponding to 6–6.6 g L^{-1} of cell dry weight (CDW), which yielded sufficient CFX for our experiments. Cells were then harvested by centrifugation at 12,000*g* for 30 min at 4°C and re-suspended in 10 mM phosphate buffer pH 7.0 (2 mL g^{-1} of cell wet weight). Then, cells were lysed in a high pressure homogenizer (Haskel, Wesel, Germany) twice at a pressure drop of 1,000 bar over the orifice at 8°C. Cell debris and insoluble components were removed by centrifugation at 25,000g for 45 min at 4°C. The supernatant was used as CFX and applied either directly or stored at −80°C. Where indicated, the CFX was further treated by washing using a centrifugation-dependent ultrafiltration unit (Sartorius, Dietikon, Switzerland) with a molecular weight cut off of 10 kDa. The buffer was exchanged by consecutive dilution and concentration steps with 10 mM phosphate buffer using a total of at least five sample volumes.

Reaction Conditions

Multi-enzyme reactions were performed in a liquid volume of 10 mL in thermostated double-jacketed beakers at 37°C. CFX was diluted into reaction buffer (final composition 100 mM $NaHCO_3$ pH 7.7; 5 mM $MgCl_2$; 0.8 mM KCl; 11.1 mM GLC; 11.1 mM sodium phosphate pH 7.7) to a final protein concentration of 1 or 10 mg mL^{-1}. NAD^+ and lactate dehydrogenase (LDH) were added to different concentrations depending on the experimental setup. Reactions were started by adding ATP to a final concentration between 2.875 and 23 mM as indicated. ATP degradation experiments were performed similarly but without GLC in the reaction buffer. Samples were taken at indicated time points and the reaction was stopped by adding an equal volume of isopropanol and immediate chilling on ice. Proteins were removed by centrifugation and the supernatant was used after appropriate dilution with water for further analysis. Experiments with $^{13}C_1$-labeled GLC were performed as described above for unlabeled GLC.

The formation of 5,6,7-trideoxy-D-threo-heptulose-1-phosphate (TDHP) was carried out in an aliquot of 10 mL (10 mg mL^{-1} CFX in 100 mM $NaHCO_3$ pH 7.7, 5 mM $MgCl_2$, 0.8 mM KCl, 0.575 mM NAD^+, 1 U mL^{-1} LDH, 11.1 mM or 55.5 mM GLC, and 11.1 or 55.5 mM sodium phosphate pH 7.0), DHAP production from GLC was started by adding ATP to a final concentration of 2.875 mM. Butanal was added to produce TDHP via a one-step or a two-step process. For a one-step process, butanal (1 mmol) and RAMA (10 U) were added before starting the reaction; for a two-step process the components were added after an initial DHAP-production phase of 30 min. Additional butanal pulses were added as described in the text.

Analytics

Protein concentrations were determined as described previously (Bradford, 1976). All mentioned CFX concentrations refer to the concentration of total protein in the reaction system. The metabolites ATP, ADP, and AMP (summarized as AXP) and DHAP were analyzed in 96-well plates using an enzymatic assay reported previously (Bergmeyer et al., 1984) but downscaled to 200 μL. GLC was analyzed using a commercial enzyme kit (R-Biopharm, Darmstadt, Germany), also downscaled to 200 μL. All these assays relied on a final measurement of the rate of NAD^+/NADH conversion based on the change in absorption at 340 nm, which was recorded on a 96-well plate reader (Perkin Elmer, Waltham, Massachusetts). The additional enzymes required for the assay were added using an automatic dispenser (Perkin Elmer). Absolute concentrations were calculated from previously prepared standard curves. In graphical representations for reactions containing 10 mg mL^{-1} of total protein, the calculated GLC concentration of 11.1 mM at addition of ATP is shown rather than the first value measured a few seconds later ($t = 0$), because the inevitable period between reaction start and first sampling was sufficient to consume substantial portions of the initially added GLC. The initial specific production rate of DHAP was determined from the period of linear increase in DHAP concentrations. All results are the average of two parallel reactions, with each reaction analyzed in triplicate so that error bars represent the standard deviation of six measurements.

The ratio between $^{12}C_1$-DHAP and $^{13}C_1$-DHAP was determined by mass spectrometry operated in the negative mode. After enzyme inactivation (see above), the sample was further diluted 1:250 in MeOH:H_2O (3:1) to give a final dilution of 1:1,000 and then analyzed by ESI-MS (MDS Sciex 4000 Q-Trap; Applied Biosystems, Foster City, CA) using continuous direct injection with a syringe pump at 30 μL min^{-1} (general settings: ion spray voltage = −4,200 V; curtain gas = 15; collision gas = 4; temperature = 200°C; ion source gas 1 = 30; ion source gas 2 = 40; values without units represent arbitrary instrument-specific units). The ^{12}C- and ^{13}C-DHAP signal was measured using the signal intensity of the phosphate fragment ($m/z = 97$) of the mother ions of ^{12}C-DHAP ($m/z = 169$) and ^{13}C-DHAP ($m/z = 170$; declustering potential = −25 V; collision energy = −14 V; cell exit potential = −15 V).

NADH stability and glucose-6-phosphate dehydrogenase (G6P-DH) activity were analyzed using the same 96-well plate reader system described above. An aliquot of 10 μL of 50 mM NADH in water was added to 200 μL of CFX (protein concentration of 1 mg mL^{-1} in 100 mM $NaHCO_3$ pH 7.7, 5 mM $MgCl_2$, 0.8 mM KCl) and absorption at 340 nm was measured every 10 s. To analyze the stability of the NAD^+ regeneration capacity, CFX (composition as before) was incubated at 37°C for different periods of time and then chilled on ice. NADH was added to aliquots of 200 μL, the reaction was incubated at 37°C for 10 min and then absorption at 340 nm was recorded. Results are the average of three parallel reactions.

The analysis of the G6P-DH activity was disturbed by remaining NADH-oxidation capacity of the CFX (see below). To circumvent this, samples were pre-incubated for 2 h at 37°C (at which temperature G6P-DH is stable; Murakami et al., 2006), but not the rest of the cellular NADH-oxidation capacity, see below). An aliquot of 10 μL of G6P (50 mM in water) was added to 200 μL of CFX (1 or 10 mg mL^{-1} in 100 mM $NaHCO_3$, pH 7.7, 5 mM $MgCl_2$, 0.8 mM KCl, and $NADP^+$ or NAD^+ as indicated) and absorption at 340 nm was measured every 5 s. The specific activity was determined by linear regression. Results are the average of three parallel reactions.

For the quantification of TDHP, for which no commercial standard was available, we synthesized the reference compound in a 1 mL aliquot from commercially available DHAP by incubation of the reaction mixture (25 mM DHAP; 100 mM butanal; 1 U mL^{-1} RAMA; in water) at 37°C for 1 h. The reaction was terminated by filtration through an ultrafiltration unit (Sartorius, Dietikon, Switzerland) with a molecular weight cut off of 10 kDa. DHAP was quantified before and after the reaction as described above, and the difference was set as the concentration of TDHP in the sample as reported previously for calculating conversion rates (Fessner and Sinerius, 1994; Wong and Whitesides, 1983). A standard curve for TDHP (in 75% MeOH; 25% water; 2 mM formic acid; 5 mM ammonium formate, 4 μM 3-(N-morpholino)propanesulfonic acid (MOPS) was recorded using ESI-MS analysis (see above). The constant signal of the phosphate fragment of TDHP ($m/z = 241$; declustering potential = −60 V; collision energy = −19 V; cell exit potential = −15 V) was normalized against the constant $m/z = 80$ fragment signal of MOPS ($m/z = 208$; declustering potential = −65 V; collision energy = −40 V; cell exit potential = −11 V) in order to compensate for day-to-day variations of total signal intensities. Samples from TDHP synthesis were diluted appropriately (in 75% MeOH; 25% water; 2 mM formic acid; 5 mM ammonium formate, 4 μM MOPS) and the normalized signal was used for quantification using the standard curve.

Results

A "System of Biotransformations" (SBT) for the Production of DHAP—A Multi-Enzyme Pathway With Balanced Cofactor Recycling Derived From *E. coli*'s Glycolysis

The enzymes of bacterial glycolysis can convert cheap GLC in vitro to a variety of interesting building blocks, in particular DHAP for the synthesis of vicinal diols (Schümperli et al., 2007). In addition to the conversion of the carbon skeleton, such a multi-enzyme route involves the consumption of cofactors such as ATP and consequently

requires cofactor regeneration. Figure 1 illustrates one possible multi-enzyme route based on *E. coli*'s glycolysis. The crucial step is the cleavage of fructose-1,6-bisphosphate (FBP, please refer to Fig. 1 for a list of abbreviations) into DHAP and glyceraldehyde-3-phosphate (GAP). In wild-type (WT) glycolysis, DHAP is isomerized by triose-phosphate-isomerase (TpiA) to GAP and enters the lower part of glycolysis. Hence, the knockout of the *tpiA* gene is essential for the accumulation of DHAP, which in turn reduces the flux through the lower part of glycolysis by a factor of two to one molecule of GAP per mole of GLC.

A theoretically cofactor-balanced enzyme system for the production of DHAP from GLC via glycolysis consists of 10 enzymatic reactions which can be grouped into 3 subsystems: (i) the upper part of glycolysis which is the production pathway from GLC to DHAP and GAP (4 reactions, 2 molecules of ATP converted to ADP); (ii) the lower part of glycolysis from GAP to PYR, building the ATP regeneration pathway (5 reactions, 1 molecule of NAD^+ converted to NADH, 1 molecule of Pi consumed, 2 molecules of ATP generated from ADP); and (iii) the LDH-based NAD^+/NADH regeneration system (1 reaction, 1 molecule of NADH converted to NAD^+). An evaluation of the thermodynamics of the SBT based on tabulated Gibbs energy values under standard conditions and at pH 7 indicates that the reaction should proceed easily to completion (data not shown).

In living cells, G6P is primarily produced during the import of GLC by the PTS, which requires PEP as a cofactor and is partly membrane-located. The application of a cell-

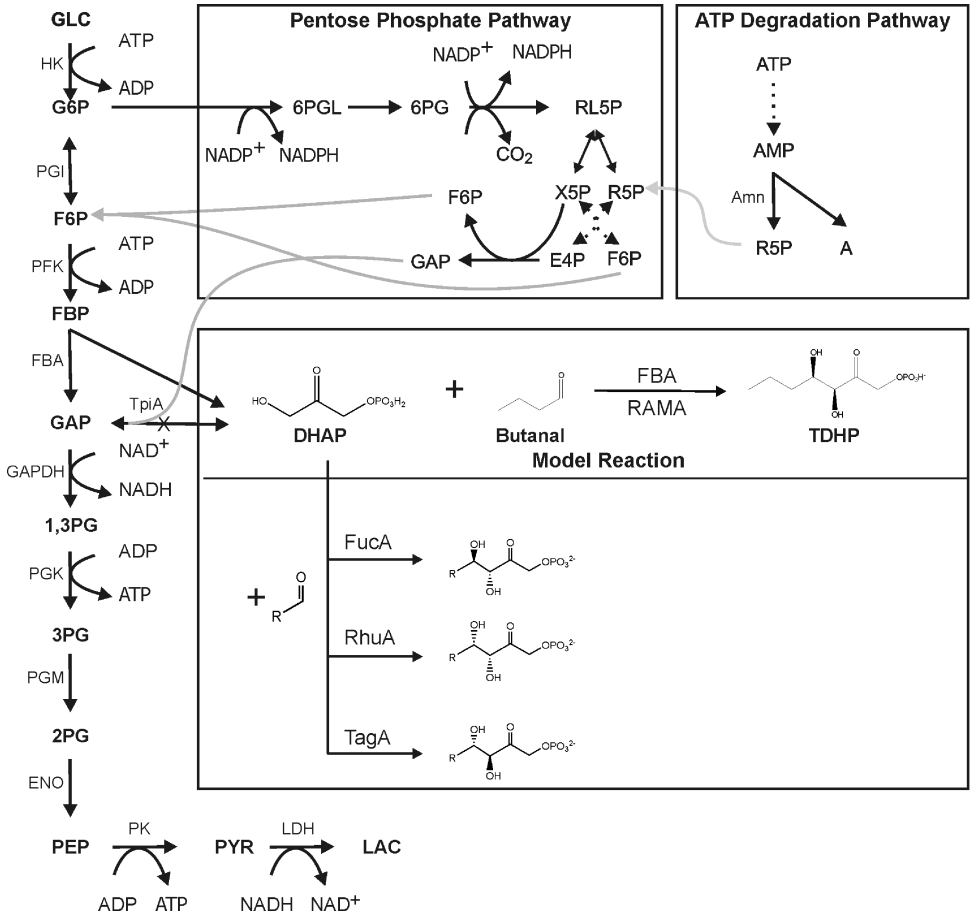

Figure 1. An SBT for unnatural carbohydrate synthesis via DHAP-dependent aldolases and a schematic overview of different routes leading to the formation of DHAP. The model reaction chosen in this study is catalyzed by FBA and RAMA. Note that TpiA is knocked in the DHAP producing SBT. Solid lines represent a single enzyme catalyzed reaction, dotted lines represent multiple reactions. HK, hexokinase; PGI, phosphoglucose isomerase; PFK, phosphofructokinase; FBA, frcuctosebisphosphate aldolase; TpiA, triosephosphate isomerase; GAPDH, glyceraldehyde-3-phosphate dehydrogenase; PGK, phosphoglycerate kinase; GPM, phosphoglycaerate mutase; ENO, enolase; PK, pyruvate kinase; LDH, lactate dehydrogenase; FucA, fuculose aldolase; RhuA, rhamnulose aldolase; TagA, tagatose aldolase; iRAMA, rabbit muscle aldolase; Amn, AMP-nucleosidase; GLC, glucose; G6P, glucose-6-phosphate; F6P, fructose-6-phosphate; FBP, fructose-1,6-bisphosphate; DHAP, dihydroxyacetone phosphate; GAP, glyceraldehyde-3-phosphate; 1,3PG, 1,3!diphosphoglycerate; 3PG, 3-phosphoglycerate; 2PG, 2-phosphoglycerate; PEP, phosphoenolpyruvate; PYR, pyruvate; LAC, lactate; 6PGL, 6-phosphogluconolactone; 6PG, 6-phospho-gluconate; RL5P, ribulose-5-phosphate; R5P, ribose-5-phosphate; X5P, xylulose-5-phosphate; E4P, erythrose-4-phosphate; A, adenine; ATP, adenosine-triphosphate; ADP, adenosine-diphosphate; AMP, adenosine-monophosphate; AXP, sum of adenosine phosphates; NAD, nicotinamide adenine dinucleotide; NADP, nicotinamide adenine dinucleotide phosphate; TDHP, 5,6,7-trideoxy-D-threo-heptulose-1-phosphate.

free system (see below) raised the question whether or not the addition of a soluble hexokinase-type of reaction (either from gene expression in the cultured strain or as an addition at the in vitro stage) is required. Literature data on the regulation of the endogenous *E. coli* glucokinase (GLK) indicated that it would be present after cultivation on yeast extract supplemented mineral medium with GLC as the carbon source (Meyer et al., 1997). We will refer to this multi-enzyme sequence for the production of DHAP with complete cofactor regeneration as the SBT.

The following parts address the general applicability of recruiting a highly interconnected pathway from central carbon metabolism for the synthetic purpose of a SBT.

Implementation of the Reaction Network

For the generation of an SBT for the production of DHAP, a *tpiA* knockout mutant was constructed in *E. coli* W3110. Since the mutant is strongly impaired in growth on mineral medium with GLC as the sole carbon source, yeast extract was added (M9-GYE). The *tpiA::kan* mutant was still hampered in growth on M9-GYE ($\mu_{max} = 0.4\,h^{-1}$ in exponential growth phase) compared to the WT strain W3110 ($\mu_{max} = 0.8\,h^{-1}$). Cultivations were carried out as fed-batch fermentations and harvested cells were homogenized to produce CFX.

To test the feasibility of DHAP accumulation in a single knockout mutant, CFX from the *tpiA* mutant was diluted to a total protein concentration of $1\,mg\,mL^{-1}$. As a control, we used CFX derived from the WT W3110 strain grown under the same conditions. To eliminate any potential limitations for DHAP production by cofactor regeneration at this stage, we added LDH ($1\,U\,mL^{-1}$) and then the cofactors (ATP: 11.5 mM and NAD^+: 5.75 mM) in half-stoichiometric amounts relative to GLC (11.1 mM). Both the WT and the *tpiA::kan* mutant-derived CFXs consumed the entire GLC provided in 125–175 min (Fig. 2A). However, only the *tpiA*-derived CFX accumulated 8.3 mM DHAP within 5 h, which was about 65-fold higher than in the WT-derived CFX (Fig. 2A). The SBT showed stable operation for a period of 10 h in a continuous system as steady-state DHAP concentrations only showed minor changes (data not shown).

In principle, the use of crude CFX could lead to the production of DHAP from sources other than GLC, such as from metabolites being present in the CFX, by degradation of macromolecules (DNA, RNA, or proteins) or along pathways other than the selected SBT. However, when the SBT was operated with $^{13}C_1$-labeled GLC, 90% of the produced DHAP was labeled, indicating that the major part of the produced DHAP was indeed derived from GLC along the SBT (Fig. 2B). Pathways leading to the formation of unlabeled DHAP are discussed in the Behavior of the SBT at High CFX Concentrations Section. Control experiments without either GLC or ATP did not produce any significant amounts of DHAP (Fig. 2C), and verified that GLC was used as the carbon source for DHAP synthesis.

Interestingly, no DHAP accumulation could be observed when NAD^+ was not added to the SBT (Fig. 2D), although ATP had been added to half-stoichiometric amounts to GLC. This indicated that the enzymatic cascade was disrupted because of the unavailability of the cofactor for glyceraldehyde-3-phosphate dehydrogenase (GAPDH). Unavailability of NAD^+ would lead to accumulation of GAP and a resulting equilibrium-induced shift of the aldolase reaction to the side of FBP. In turn, this result suggested that in the presence of NAD^+ the regeneration pathway in the lower part of glycolysis was both, functional and essential for DHAP accumulation. However, the addition of LDH for the regeneration of NAD^+ from NADH did not appear to be essential for the system's performance, because DHAP formation occurred independently of LDH addition (see below for a more detailed analysis).

Behavior of the SBT at High CFX Concentrations

In order to reduce the reaction time of 5 h until maximum DHAP concentrations were reached (Fig. 2A) the total protein concentration of CFX was increased from 1 to $10\,mg\,mL^{-1}$. As expected, the time until maximum DHAP concentrations was reduced significantly to 30 min (Fig. 3A).

However, in contrast to the observations with CFX concentrations of $1\,mg\,mL^{-1}$, a substantial 46% of the DHAP produced were not labeled when the experiment was carried out with $^{13}C_1$-labeled GLC (Fig. 3B). In addition, significant amounts of DHAP were produced in experiments that contained either GLC but no ATP or ATP but no GLC (Fig. 3C). The latter experiments indicated that there were previously unconsidered substrates and pathways for the production of DHAP, which had remained unnoticed previously because of the high dilution of the CFX (appr. 200- to 300-fold based on intracellular protein concentration; Cayley et al., 1991). In this set of experiments, the dilution of CFX was 10-fold less, and based on published intracellular metabolite concentrations (Bennett et al., 2009), ATP and NAD^+ concentrations in a 30-fold dilution can be expected to be in the range of 0.3 and 0.1 mM, respectively. This would explain GLC consumption and DHAP production without addition of extra ATP (Fig. 3C) or NAD^+ (Fig. 3D).

Unlabeled DHAP could be produced from non-GLC sources, from GLC via the pentose–phosphate pathway (PPP; Fig. 1) or by losing its label after synthesis. We could not identify any biochemical reaction for the latter route from the literature. Production via the PPP would require a transfer of reduction equivalents from NADH to $NADP^+$, probably via the transhydrogenase UdhA (Boonstra et al., 1999; Sauer et al., 2004), because the first enzymes of the PPP depend exclusively on NADPH (Fuhrer and Sauer, 2009).

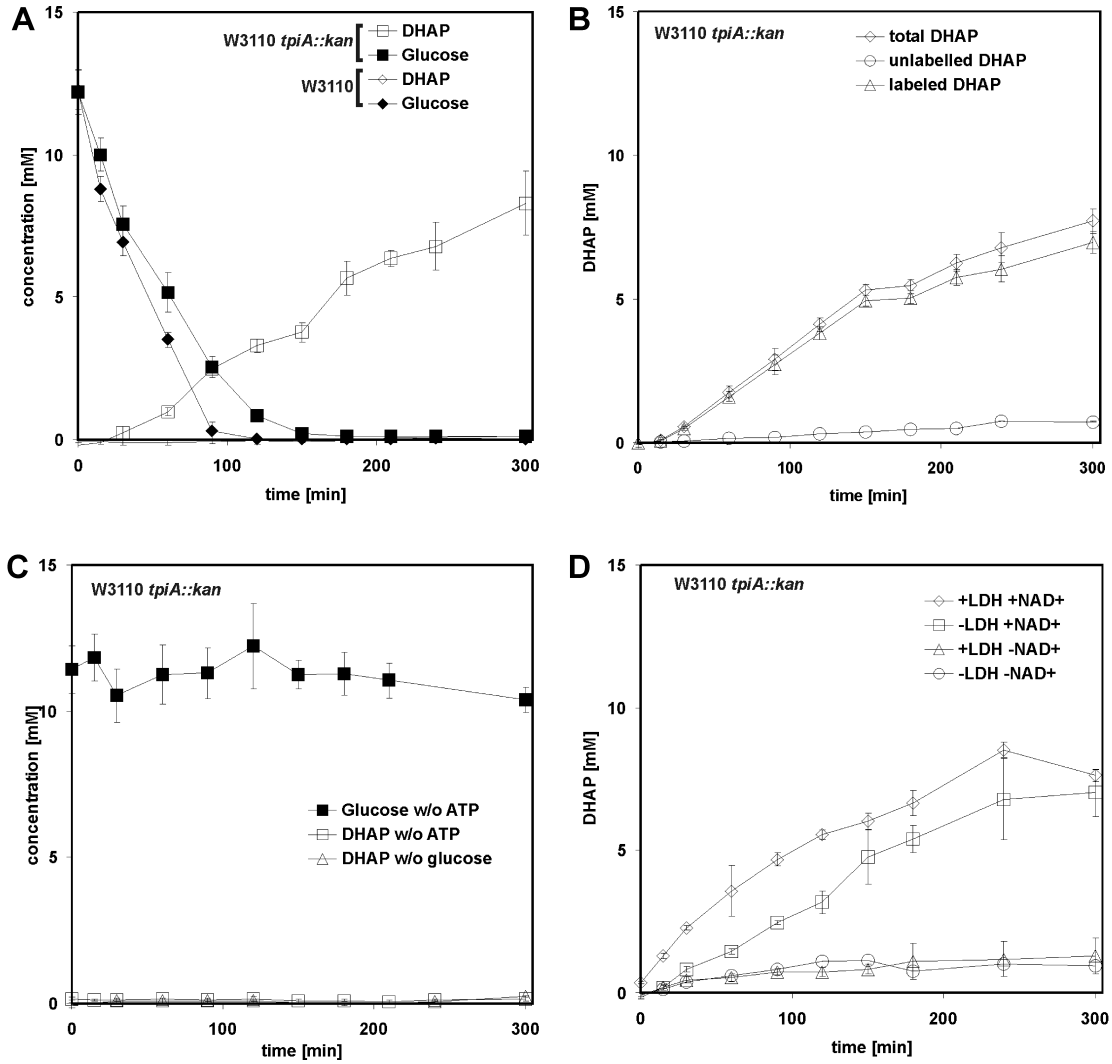

Figure 2. The impact of process conditions and the genetic background on DHAP production using CFX with a total protein concentration of 1 mg mL^{-1}. **A**: Comparison of DHAP production and glucose consumption in WT- and *tpiA::kan*-derived CFXs. **B**: Analysis of the origin of DHAP using $^{13}C_1$-glucose. **C**: DHAP production in CFX in the absence of glucose or ATP. **D**: Production of DHAP in the presence and absence of additional NAD^+ and LDH.

Via this route, the $^{13}C_1$-label of GLC could be released as CO_2 by 6-phosphogluconate dehydrogenase (GND) and would be no longer present in the subsequent PPP intermediate fructose-6-phosphate (F6P), from which DHAP could be formed along SBT reactions (Fig. 1).

In order to obtain an estimate of GLC flux through the PPP, we analyzed representatively the activity of G6P-DH under operating conditions of the reaction network. Under low nicotinamide adenine dinucleotide conditions (1 mM), G6P-DH activity was only high when $NADP^+$ was supplied in control experiments, not when NAD^+ was supplied. When 5.75 mM NAD^+ was added to the reaction mixture, G6P-DH activity was observed, but only at a high protein concentration of 10 mg mL^{-1}. At lower NAD^+ concentrations G6P-DH activity was reduced and no activity was observed in the absence of NAD^+ (Table I). Consequently, it seems likely that a fraction of the unlabeled DHAP under high protein and high NAD^+ conditions is still derived from GLC but formed after channeling a part of the GLC through the PPP. However, even under these conditions, the G6P-DH reaction rate was eightfold lower in our assay than the initial specific DHAP production rate in the corresponding DHAP-production experiment, pointing strongly to another source of unlabeled DHAP.

Debugging of the Reaction Network for High CFX Concentrations

As a substitute for GLC, compounds present in the CFX or ATP itself could theoretically serve as sources for DHAP. The initial ATP supply was varied by a factor of two in order

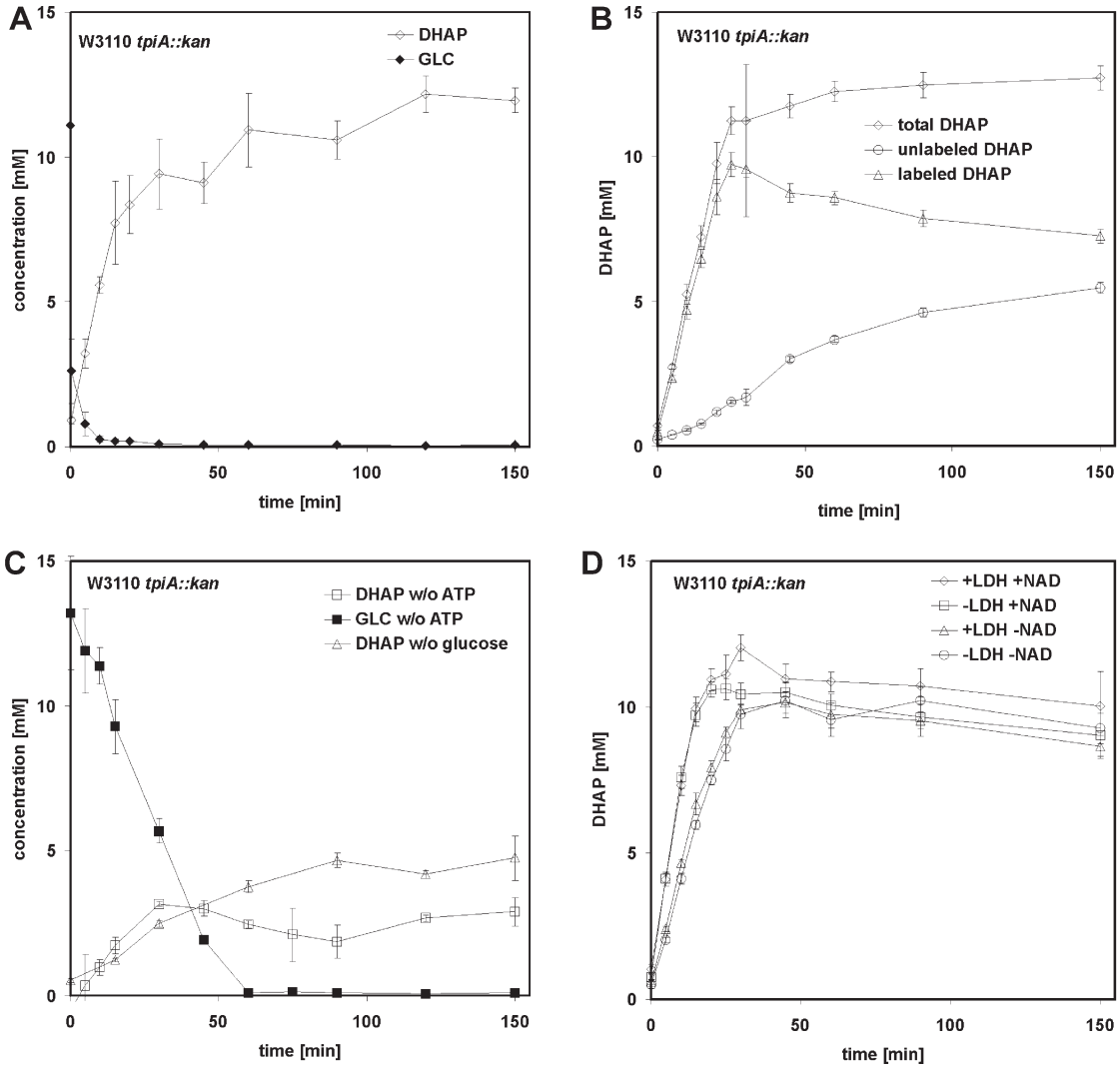

Figure 3. Acceleration of DHAP production by using CFX with a protein concentration of 10 mg mL^{-1}. **A**: DHAP production and glucose consumption. **B**: Analysis of the origin of DHAP using $^{13}C_1$-GLC. **C**: DHAP production in the absence of glucose or ATP. **D**: Production of DHAP in the presence and absence of additional NAD^+ and LDH.

to determine the impact of initial ATP concentrations onto DHAP formation in the absence of GLC. The time course of DHAP-production showed a functional relationship to the initial ATP concentration. Varying the initial ATP concentration between 23 and 5.75 mM led to a corresponding variation in the final DHAP concentration (Fig. 4A), but the yield of DHAP per added ATP remained nearly constant (0.70, 0.66, and 0.63 mol mol^{-1} for initial ATP concentrations of 23, 11.5, and 5.75 mM, respectively). This was a strong indication that ATP was a main substrate for DHAP production in the absence of GLC.

Table I. G6P-DH activity under operating conditions of the system and reduced NAD^+ concentrations using two different dilutions of the CFX.

	Protein conc. mg mL^{-1}	Specific G6P-DH activity μmol min^{-1} g protein^{-1}
1 mM $NADP^+$	1[a]	71 ± 4
5.75 mM NAD^+	1[a]	<0.1
5.75 mM NAD^+	10[b]	6 ± 0.4
0.575 mM NAD^+	10[b]	1 ± 0.1
0.0575 mM NAD^+	10[b]	0.4 ± 0.01
w/o NAD^+	10[b]	<0.1

[a]Approximately corresponding to a dilution of 1:300.
[b]Approximately corresponding to a dilution of 1:30.

A potential ATP degradation pathway leading to DHAP as the final product consists of dephosphorylation of ATP to AMP and subsequent hydrolysis by AMP-nucleosidase (Amn) to ribose-5-phosphate (R5P) and adenine (A; Fig. 1), the first step in the primary AMP degradation pathway (Leung and Schramm, 1980). R5P can then enter the PPP, where three molecules of R5P (two of which are first converted to xylulose-5-phosphate by PPP enzymes) can lead to two molecules of F6P and one molecule of GAP. In a further step, F6P could be phosphorylated to FBP, which

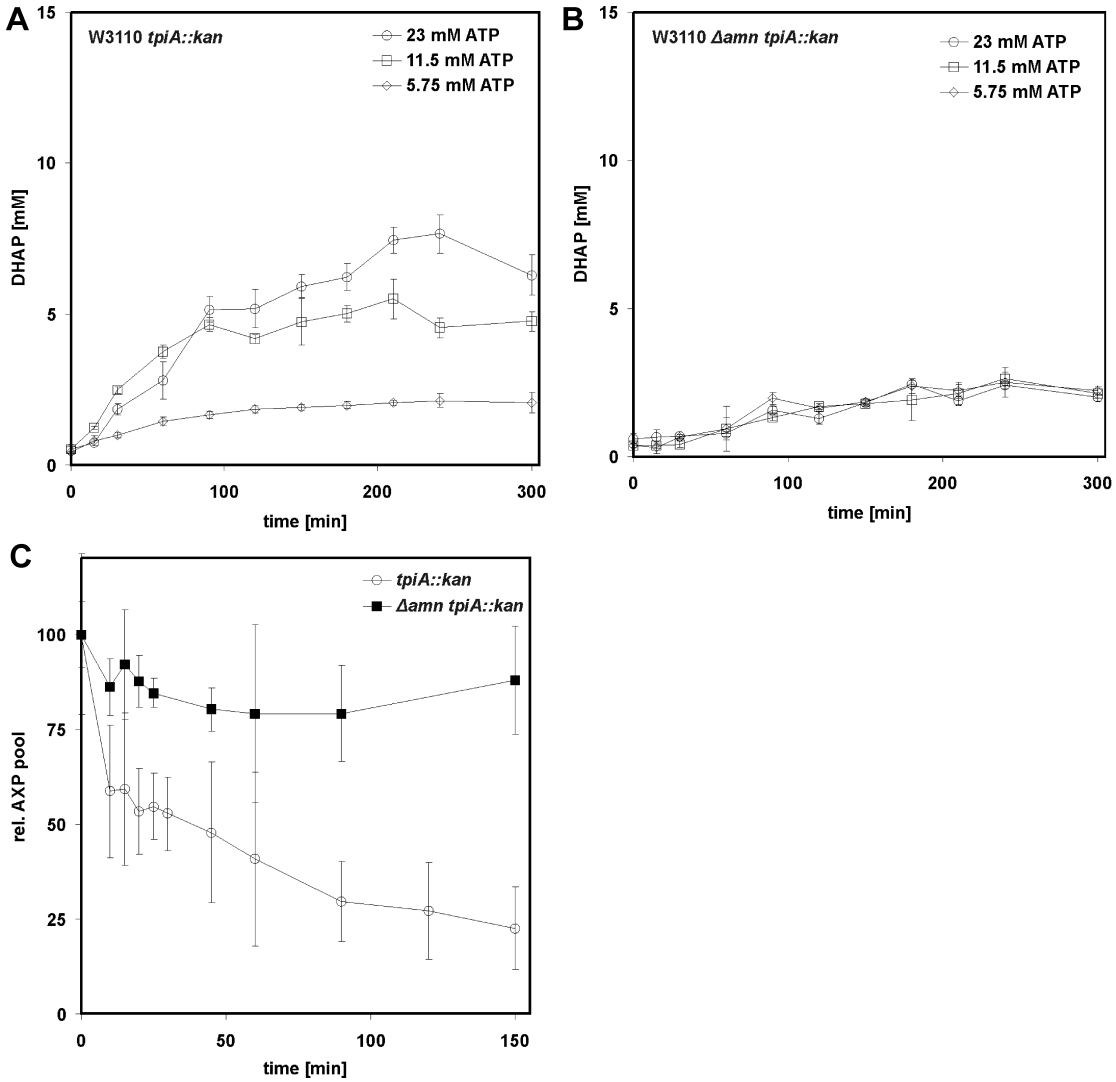

Figure 4. Debugging of the reaction cascade: removing DHAP production from ATP and stabilization of AXP pools using 10 mg mL^{-1} protein concentration. **A**: Effect of different initial ATP concentrations on DHAP production without glucose using *tpiA::kan*-derived CFX and (**B**) using Δ*amn tpiA::kan*-derived CFX. **C**: The relative amount of ATP, ADP, and AMP in a GLC metabolizing experiment was analyzed over the time course of the reaction using *tpiA::kan*- or Δ*amn tpiA::kan*-derived CFX.

could then be converted to DHAP and GAP. The ADP produced in the latter step could then be re-generated in the lower glycolysis (Fig. 1). Taking stoichiometric coefficients into account, this would lead to the following overall reaction stoichiometry:

$$3\mathrm{ATP} \rightarrow 2\mathrm{DHAP} + 2\mathrm{GAP} + \mathrm{PYR} + 3\mathrm{A} + 5P_\mathrm{i}$$

This corresponds to a theoretical yield of $Y_{\mathrm{DHAP/ATP}}$ of 0.66 mol mol^{-1}, which is close to the observed yields for the different initial ATP concentrations (Fig. 4A).

Because of this strong indication, a Δ*amn tpiA::kan* knockout strain was constructed, which showed the same growth deficient phenotype as the *tpiA::kan* single mutant ($\mu_{\max} = 0.4\,\mathrm{h}^{-1}$). In fact, the CFX derived from a Δ*amn tpiA::kan* double knockout strain produced only low amounts of DHAP, if GLC was not present and no longer showed a functional relationship between initial ATP supply and final DHAP concentrations (Fig. 4B) supporting the notion that the prevention of Amn production disrupted the pathway from ATP to DHAP. Finally, the AXP pool (the sum of the concentrations of ATP, ADP, and AMP) could be stabilized by introducing this gene deletion: the conversion of GLC to DHAP in a Δ*amn tpiA::kan* mutant proceeded with an AXP pool that was—within the limits of measurement—stable, while the pool decreased to about 25% when CFX produced from a strain without the *amn* mutation was used (Fig. 4C). Remarkably, the specific initial DHAP production rate from GLC increased from $47 \pm 2\,\mu\mathrm{mol\,min^{-1}\,g^{-1}}$ of protein for *tpiA::kan*-derived CFX to $80 \pm 2\,\mu\mathrm{mol\,min^{-1}\,g^{-1}}$ of protein for Δ*amn tpiA::kan*-derived CFX. However, introducing the *amn*

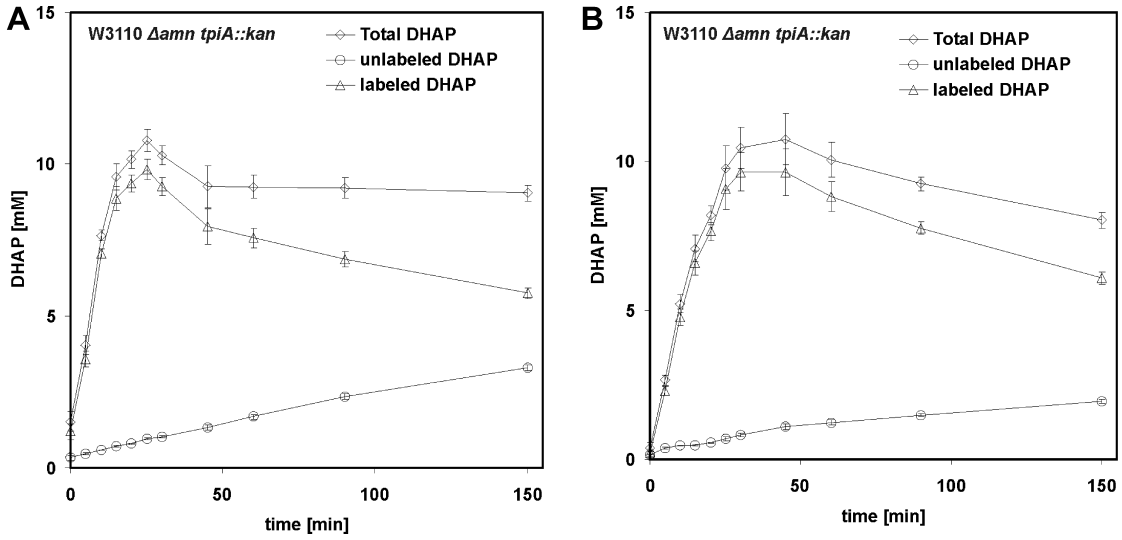

Figure 5. Analysis of the origin of DHAP using $^{13}C_1$-GLC using 10 mg mL^{-1} of CFX derived from Δ*amn tpiA::kan*-double mutant strains, either not washed (**A**) or washed (**B**).

deletion into a *tpiA*-deficient strain did not completely abolish DHAP production from other sources than GLC.

Production of Unlabeled DHAP in the Δ*amn tpiA::kan* Double Mutant

In order to comprehensively address the question of how much DHAP is produced from GLC; $^{13}C_1$-labeled GLC was again supplied as substrate in an SBT using CFX from the double mutant. Although the amount of unlabeled DHAP decreased (Fig. 5A), unlabeled DHAP still contributed substantially to the total amount and still exceeded the amount that should theoretically have been produced after passing G6P through the PPP instead of glycolysis. To exclude that the unlabeled DHAP could simply be a result of the conversion of metabolites still available from the CFX-preparation, the CFX was washed prior to application. This reduced the amount of unlabeled DHAP to about 25% of total DHAP produced (Fig. 5B) and indicated that a certain amount of unlabeled DHAP using unwashed CFX has a metabolite origin with a molecular weight <10 kDa. This could also explain GLC consumption and DHAP production in the absence of ATP (Fig. 3C). Finally, we cannot exclude that degradation products from macromolecules >10 kDa, in particular of RNA, also contribute to the formation of unlabeled DHAP.

In summary, these results illustrate the complexity of using CFXs, especially if high CFX concentrations are applied, and indicate three sources for potentially interfering reactions: (i) cofactors supplied for SBT operation are used for different purposes (DHAP formation from ATP); (ii) utilization for formerly cytosolic small molecules (reduction in DHAP formation when using washed CFX, GLC consumption in the absence of ATP); and (iii) degradation products from macromolecules as substrates.

From Stoichiometric to Catalytic Operation—Optimization of ATP Concentrations

The design of the reaction network theoretically contains a complete recycling system for ATP and NADH if no parallel reactions take place. Hence, catalytic amounts of ATP should be sufficient for a nearly complete conversion of GLC to DHAP and lactate. The production of DHAP at a CFX concentration of 10 mg mL^{-1} using reduced initial ATP concentrations was analyzed and compared between *tpiA::kan*-and Δ*amn tpiA::kan*-derived CFX in order to investigate the impact of *amn* deletion onto the overall production capacity and to find the minimal ATP concentration for sustained DHAP production.

Absolute DHAP concentrations were similar with a *tpiA::kan*- and Δ*amn tpiA::kan*-derived CFX, if 11.5 mM ATP were supplied. A reduction of the initial ATP supply showed a strong impact onto DHAP production when *tpiA::kan*-derived CFX was used, but not when Δ*amn tpiA::kan*-derived CFX was used (Table II). These results showed again the benefit of the *amn* knockout, which enabled the use of 2.875 mM ATP for sustained DHAP production, which is only 15% of the amount of ATP that would be required to stoichiometrically produce the same amount of DHAP from GLC without ATP regeneration.

Table II. The impact of reduced initial ATP concentrations on maximal DHAP production in *tpiA::kan*- and Δ*amn tpiA::kan*-derived CFX.

	Maximum DHAP conc. (mM)	
ATP conc. (mM)	*tpiA::kan* CFX	Δ*amn tpiA::kan* CFX
11.50	12	11.8
5.75	9	11
2.875	5.8	9.7

Optimization of Cofactor Concentrations—NAD^+ and the Role of LDH

NAD^+ is required for the conversion of GAP to 1,3PG, which is the first reaction for the regeneration of ATP in the lower part of glycolysis. From the previously discussed experiments, it was clear that (i) the regeneration pathway was essential for DHAP production (Fig. 2D); and (ii) NAD^+, but not LDH, was required if CFX at 1 mg mL^{-1} was used (Fig. 2D); furthermore, in experiments with high CFX concentration (10 mg mL^{-1}), neither NAD^+ nor LDH were required (Fig. 3D), presumably because NAD^+ amounts present in the CFX were enough for GAPDH activity.

The expandability of LDH for NAD^+ regeneration shown earlier suggested the presence of alternative enzymes in the CFX, which could regenerate NADH to NAD^+. Analyzing the stability of NADH in CFX confirmed that NADH was rapidly oxidized (Fig. 6A), with a specific rate of approximately 260 μmol min^{-1} g^{-1} of total protein in CFX. Within 2.5 min, the NADH concentration was reduced from 1 to approximately 0.25 mM, when it stopped abruptly; presumably because of temperature sensitivity (see below). This catalytic activity is actually sufficient for an efficient regeneration of NAD^+, since NADH is produced at a maximum specific rate of 80 μmol min^{-1} g^{-1} as calculated on the basis of our maximum DHAP production rate using the Δ*amn tpiA::kan* system and 10 mg mL^{-1} of protein.

We also analyzed the NAD^+ regeneration capacity after incubation of CFX for different periods of time at 37°C in order to verify that the NAD^+ regeneration capacity was maintained sufficiently long. CFX with a protein concentration of 1 mg mL^{-1} was incubated at 37°C for 15–120 min, then NADH was added and its concentration after 10-min incubation at 37°C was determined. The analysis showed

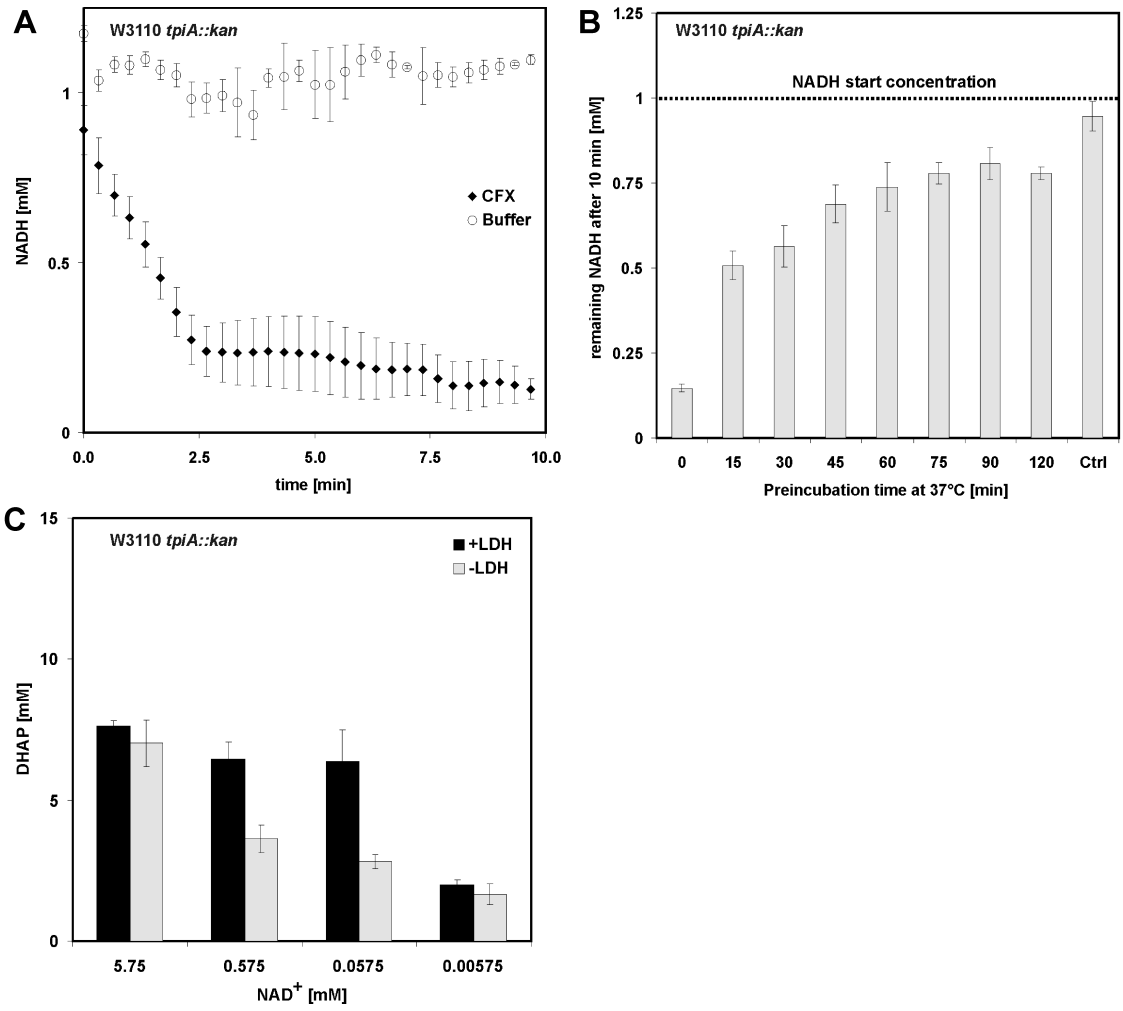

Figure 6. NADH degradation capacity of CFX and optimization of NAD^+ concentrations for experiments using 1 mg mL^{-1} of CFX. **A**: NADH stability in *tpiA::kan*-derived CFX at 1 mg mL^{-1}. 1 mM NADH was added to CFX and its degradation was monitored. **B**: NADH stability in *tpiA::kan*-derived CFX over time at 1 mg mL^{-1}. CFX was pre-incubated at 37°C for the indicated periods of time, then NADH was added and its concentration after 10 min was determined. Ctrl: reaction buffer without CFX. **C**: Effect of reduced NAD^+ concentrations on DHAP production in the presence and absence of LDH.

that the NADH oxidization capacity of the CFX decreased over time (Fig. 6B). After 15-min incubation of the CFX at 37°C, the capacity to oxidize NADH was reduced by about 75%, and after 60 min, NADH was almost completely stable. These results agree well with the results displayed in Figure 3D, where LDH could be completely omitted—apparently, its originally intended role was fulfilled by the remaining NADH-oxidation activities in the CFX.

However, this could not be expected for prolonged experiments such as DHAP formation at lower protein concentrations. Therefore, we determined the minimum NAD^+ concentration in the presence and absence of LDH for 1 mg mL^{-1} CFX. NAD^+ could be reduced by a factor of 100 if LDH was present, while a reduction of NAD^+ by a factor of only 10 in the absence of LDH led to already 50% less DHAP at the end of the experiment. A 1,000-fold reduction in NAD^+ impaired DHAP production regardless of the addition of LDH (Fig. 6C). This was presumably because the concentration of NAD^+ decreased to almost a 10th of the K_m value of GAPDH ($K_m = 0.045$ mM; Eyschen et al., 1999), making this reaction the bottleneck in ATP regeneration.

Without considering any follow up reactions (see below), the entire system could be operated with an ATP supply of 2.875 mM and without the addition of NAD^+ and LDH if a total protein concentration of 10 mg mL^{-1} was used.

Monosaccharide Synthesis

Since DHAP is an unstable molecule (Hettwer et al., 2002), it is not an optimal end-product of the reaction cascade. It should be rather used as a versatile building block for carbohydrate synthesis in an aldolase catalyzed reaction, for example, with RAMA (Fig. 1). To confirm that the SBT can work effectively for preparative sugar synthesis, the aldolase-catalyzed conversion of DHAP and butanal to TDHP was chosen as a model reaction, since butanal is known as a good substrate for RAMA and RAMA introduces the same stereoconfiguration of vicinal diols as *E. coli*'s fructose-bisphosphate-aldolase (FbaA; Bednarski et al., 1989) which is the primarily used aldolase in *E. coli* grown on GLC as substrate (Scamuffa and Caprioli, 1980). The latter enzyme is supposed to accept only a very limited range of aldehydes other than GAP (Fessner and Walter, 1996), which would be an asset for using the DHAP-production cascade with aldolases that produce a different stereoconfiguration. However, at this preliminary stage we used only RAMA in order to avoid any compromising of the diastereoselectivity of the produced monosaccharide.

In a first step, DHAP was produced from GLC (11.1 mM) using Δ*amn tpiA::kan*-derived CFX and only catalytic amounts of ATP (2.875 mM ATP, 10 mg mL^{-1} CFX). After an initial DHAP production phase of 30 min, butanal was added for the production of TDHP using *E. coli*'s endogenous aldolase FbaA. However, 50% of the initial DHAP was converted to TDHP within 90 min (Fig. 7A), indicating that the *E. coli* aldolase could accept butanal as aldehyde.

In order to obtain higher TDHP concentrations and faster conversion of DHAP to TDHP, the amount of GLC was increased by a factor of five (55.5 mM) and RAMA was added while maintaining the ATP concentration constant (2.875 mM). A one-step and a two-step process were used to produce TDHP. Aldolase and butanal were either added after an initial DHAP production phase (two-step, Fig. 7B) or were present from the beginning (one-step, Fig. 7C). A clear benefit of an additional butanal pulse was observed, indicated by an increase of TDHP directly after the pulse (Fig. 7B and C). However, in both cases the reaction stopped before the entire amount of DHAP was depleted as reported previously (Schoevaart et al., 1999). Similar concentrations of DHAP (~5 mM) and TDHP (~23 mM) for the one- and two-step process suggest that complete conversion of DHAP to TDHP was limited by the thermodynamic equilibrium between butanal, DHAP, and TDHP, which is known to be less favorable for synthesis than the equilibrium between DHAP, GAP, and FBP (Schoevaart et al., 1999).

Discussion

The implementation of an efficient DHAP production system for the production of an unnatural monosaccharide based on *E. coli*'s modified glycolysis demonstrates that it is easily possible to recruit in vitro a sufficiently insulated SBT from an in vivo highly interconnected metabolic network such as central carbon metabolism. GLC could be converted to DHAP using CFX from a *tpiA* knockout strain, which bisects the flux in the lower part of glycolysis. One equivalent of DHAP could be produced per equivalent of GLC and the remaining carbon backbone was used for cofactor regeneration enabling the use of catalytic concentrations of ATP and NAD^+. This potentially opens access to a large number of interesting building blocks for fine chemistry.

The high yield of DHAP on GLC and the high degree of ADP recycling indicate that only few intermediates of the SBT entered anabolic pathways in the cell. A detailed analysis of this phenomenon will be subject of a separate investigation but the major reasons for this apparent insulation can be expected to be the 30- and 300-fold dilution, which reduces the concentrations of remaining intracellular metabolites and cofactors below relevant levels in the CFX, and the fact that the complex growth medium suppresses the expression of a large number of potentially interfering genes. These overarching considerations are complemented by a number of system-specific considerations, for example, the fact that NADH concentrations in the discussed SBT were constantly low, reducing the potential for DHAP removal through the glycerol-3-phosphate dehydrogenase (GpsA), and the stoichiometric addition of phosphate led to inhibition of the methylglyoxal synthase (MgsA; Hopper and Cooper, 1971).

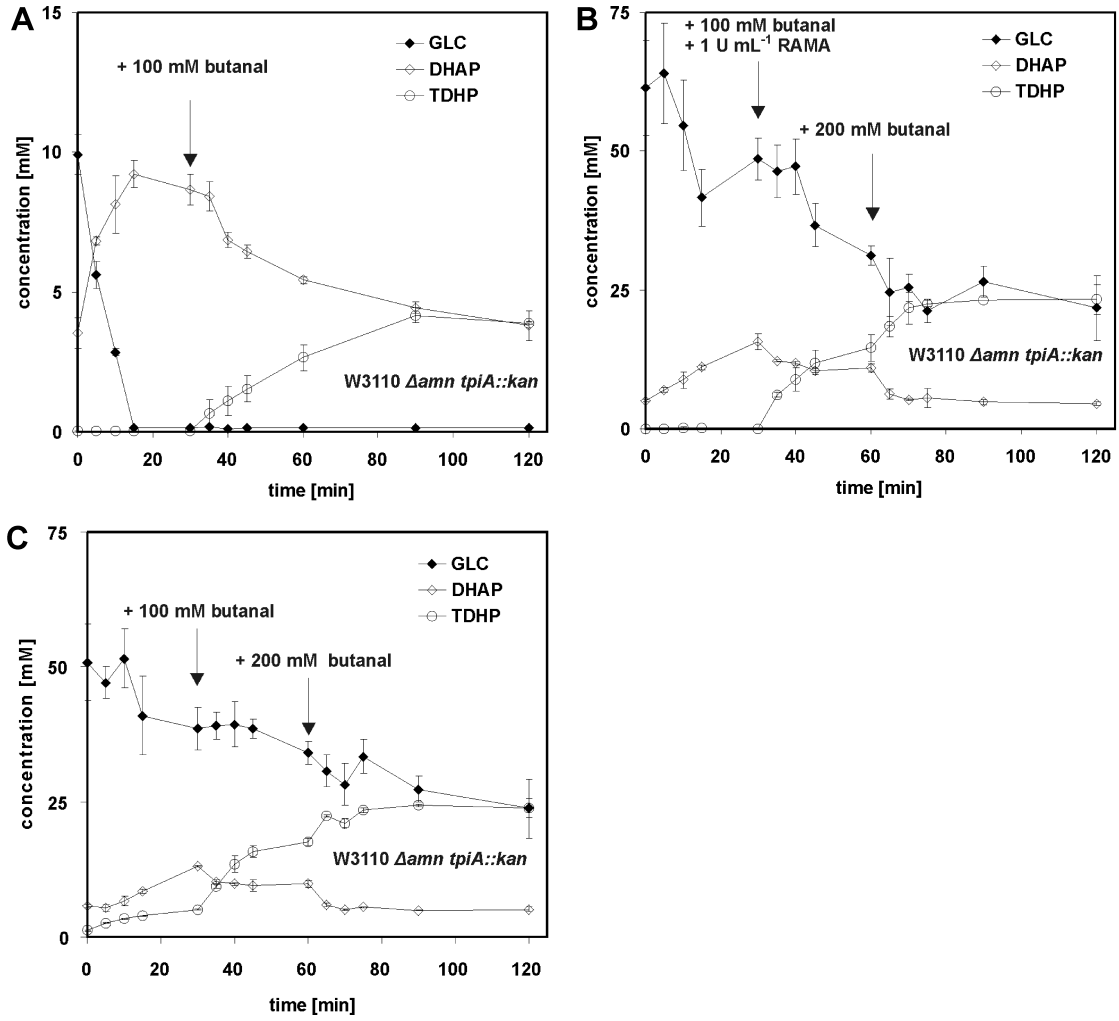

Figure 7. Production of 5,6,7-trideoxy-D-threo-heptulose-1-phosphate (TDHP) from GLC and butanal. **A**: Production of TDHP from 11.1 mM GLC in a two-step process using FBA from *E. coli*. **B**: Acceleration of TDHP production from 11.1 mM GLC in a two-step process by adding RAMA and an additional butanal pulse. **C**: Two-step process for TDHP production from 55.5 mM GLC using RAMA and two butanal pulses. **D**: Production of TDHP in a one-step process with RAMA and butanal present at the beginning of the reaction.

Another major concern was the regeneration of ATP, which was impaired by ATP degradation through enzymes that were not part of the pathway. Deletion of the *amn* gene reduced this effect substantially. Amn was recently shown to be involved in maintaining intracellular ATP levels: its deletion resulted in elevated ATP levels because the degradation pathway of AMP was impaired (Morrison and Shain, 2008). Although the conversion of ATP to ADP and AMP can still occur, it will probably occur more slowly in an *amn* mutant, since AMP is not constantly removed from the system. Consequently, the improved system's performance of the CFX derived from the *amn* mutant can be explained by an increased availability of ATP. In addition to the effect of Amn, ATP is dephosphorylated to ADP and AMP, presumably by phosphatases and other ATP metabolizing reactions, which is a well-known phenomenon in CFX-based systems (Kim and Choi, 2000). Providing energy in the form of ATP to cell-free systems is a general problem and several energy sources have been used in order to improve performance and to reduce costs (Kim and Swartz, 2000; Kim et al., 2008). Although ATP regeneration operated rather efficiently in the glycolysis-based SBT, it did not achieve complete regeneration. To address this problem, we are currently working on the comprehensive analysis of major phosphatase activities in CFX in order to design an improved strain for cell-free applications.

Finally, a future concern over the implementation of SBTs might originate from two potentially contradicting requirements: on one hand, an insulated SBT requires the absence of specific enzyme activities—in the case discussed here, for example, TpiA—while the cheap production of the CFX by cultivation (e.g., by growth on a mineral medium with a cheap carbon source) requires the presence of these activities. Generally, *tpiA* knockout strains show a growth

defect on GLC-mineral medium (Fong and Palsson, 2004; Fong et al., 2006) due to the bisection of glycolytic intermediates downstream of FBP and the resulting reduced flux of metabolites through the lower part of glycolysis (Fong et al., 2006) and the production of methylglyoxal which is toxic for the cell (Ferguson et al., 1998). In this study, the growth impaired phenotype was partly compensated by adding yeast extract to the culture which allowed slow growth. However, to generalize the concept of insulating complex pathways from CFXs, a simple knockout strategy might no longer be feasible, not least of all because multiple knockouts might lead to a lethal phenotype that cannot be recovered by medium engineering. In order to solve this problem, strategies for the simple but selective removal of specific enzyme activities are currently under investigation in our laboratory.

The authors would like to thank Anne Kümmel and Martin Held for helpful discussions, the teams at DSM Research (Jülich, Germany) and the group of Uwe Sauer (ETHZ) for help with gene knockouts, and Marco Oldiges and Christian Wandrey (Research Center Jülich) for help with setting up the MS-analysis. This work was supported by the EU-FP6 project "EUROBIOISYN".

References

Baba T, Ara T, Hasegawa M, Takai Y, Okumura Y, Baba M, Datsenko KA, Tomita M, Wanner BL, Mori H. 2006. Construction of *Escherichia coli* K-12 in-frame, single-gene knockout mutants: The Keio collection. Mol Syst Biol 2: 2006.0008.

Bednarski MD, Simon ES, Bischofberger N, Fessner WD, Kim MJ, Lees W, Saito T, Waldmann H, Whitesides GM. 1989. Rabbit muscle aldolase as a catalyst in organic synthesis. J Am Chem Soc 111(2):627–635.

Bennett BD, Kimball EH, Gao M, Osterhout R, Van Dien SJ, Rabinowitz JD. 2009. Absolute metabolite concentrations and implied enzyme active site occupancy in *Escherichia coli*. Nat Chem Biol 5(8):593–599.

Bergmeyer HU, Bergmeyer J, Grassl M. 1984. Methods of enzymatic analysis. Weinheim: VCH Verlagsgesellschaft.

Boonstra B, French CE, Wainwright I, Bruce NC. 1999. The udhA gene of *Escherichia coli* encodes a soluble pyridine nucleotide transhydrogenase. J Bacteriol 181(3):1030–1034.

Bradford MM. 1976. A rapid and sensitive method for the quantitation of microgram quantities of protein utilizing the principle of protein-dye binding. Anal Biochem 72:248–254.

Calhoun KA, Swartz JR. 2006. Total amino acid stabilization during cell-free protein synthesis reactions. J Biotechnol 123(2):193–203.

Cayley S, Lewis BA, Guttman HJ, Record MT. 1991. Characterization of the cytoplasm of *Escherichia coli* K-12 as a function of external osmolarity: Implications for protein–DNA interactions in vivo. J Mol Biol 222(2): 281–300.

Datsenko KA, Wanner BL. 2000. One-step inactivation of chromosomal genes in *Escherichia coli* K-12 using PCR products. Proc Natl Acad Sci USA 97(12):6640–6645.

Enders D, Hüttl MRM, Niemeier O. 2008. Biomimetic organocatalytic C–C-bond formations. In: Reetz MT, Lis B, Jarcoch S, Weinmann H, editors. Organocatalysis. Ernst Schering Foundation Symposium Proceedings, Vol. 2, 45–124.

Eyschen J, Vitoux B, Marraud M, Cung MT, Branlant G. 1999. Engineered glycolytic glyceraldehyde-3-phosphate dehydrogenase binds the anti conformation of NAD+ nicotinamide but does not experience A-specific hydride transfer. Arch Biochem Biophys 364(2):219–227.

Ferguson GP, Tötemeyer S, MacLean MJ, Booth IR. 1998. Methylglyoxal production in bacteria: Suicide or survival? Arch Microbiol 170(4): 209–218.

Fessner W-D, Sinerius G. 1994. Synthesis of dihydroxyacetone phosphate (and isosteric analogues) by enzymatic oxidation; sugars from glycerol. Angew Chem Int Ed Engl 33(2):209–212.

Fessner W-D, Walter C. 1992. "Artificial metabolism" for the asymmetric one-pot synthesis of branched-chain saccharides. Angew Chem Int Ed Engl 31(5):614–616.

Fessner W-D, Walter C. 1996. Enzymatic C–C bond formation in asymmetric synthesis. Topics in current chemistry Berlin, Heidelberg: Springer Verlag, p 98–194.

Fong SS, Palsson BO. 2004. Metabolic gene-deletion strains of *Escherichia coli* evolve to computationally predicted growth phenotypes. Nat Genet 36(10):1056–1058.

Fong SS, Nanchen A, Palsson BO, Sauer U. 2006. Latent pathway activation and increased pathway capacity enable *Escherichia coli* adaptation to loss of key metabolic enzymes. J Biol Chem 281(12):8024–8033.

Forster AC, Church GM. 2007. Synthetic biology projects in vitro. Genome Res 17(1):1–6.

Fuhrer T, Sauer U. 2009. Different biochemical mechanisms ensure network-wide balancing of reducing equivalents in microbial metabolism. J Bacteriol 191(7):2112–2121.

Herk Tv, Hartog AF, Babich L, Schoemaker HE, Wever R. 2009. Improvement of an acid phosphatase/DHAP-dependent aldolase cascade reaction by using directed evolution. Chem Bio Chem 10(13):2230–2235.

Hettwer J, Oldenburg H, Flaschel E. 2002. Enzymic routes to dihydroxyacetone phosphate or immediate precursors. J Mol Catalysis B Enzymatic 19(19–20):215–222.

Hold C, Panke S. 2009. Towards the engineering of in vitro systems. J R Soc Interface 6:15.

Hopper DJ, Cooper RA. 1971. The regulation of *Escherichia coli* methylglyoxal synthase; A new control site in glycolysis? FEBS Lett 13(4):213–216.

Jewett MC, Calhoun KA, Voloshin A, Wuu JJ, Swartz JR. 2008. An integrated cell-free metabolic platform for protein production and synthetic biology. Mol Syst Biol 4:220.

Kim RG, Choi CY. 2000. Expression-independent consumption of substrates in cell-free expression system from *Escherichia coli*. J Biotechnol 84(1):27–32.

Kim D-M, Swartz JR. 2000. Prolonging cell-free protein synthesis by selective reagent additions. Biotechnol Progr 16(3):385–390.

Kim DM, Swartz JR. 2001. Regeneration of adenosine triphosphate from glycolytic intermediates for cell-free protein synthesis. Biotechnol Bioeng 74(4):309–316.

Kim HC, Kim TW, Park CG, Oh IS, Park K, Kim DM. 2008. Continuous cell-free protein synthesis using glycolytic intermediates as energy sources. J Microbiol Biotechnol 18(5):885–888.

Knapp KG, Goerke AR, Swartz JR. 2007. Cell-free synthesis of proteins that require disulfide bonds using glucose as an energy source. Biotechnol Bioeng 97(4):901–908.

Leung HB, Schramm VL. 1980. Adenylate degradation in *Escherichia coli*. The role of AMP nucleosidase and properties of the purified enzyme. J Biol Chem 255(22):10867–10874.

Meyer D, Schneider-Fresenius C, Horlacher R, Peist R, Boos W. 1997. Molecular characterization of glucokinase from *Escherichia coli* K-12. J Bacteriol 179(4):1298–1306.

Meyer A, Pellaux R, Panke S. 2007. Bioengineering novel *in vitro* metabolic pathways using synthetic biology. Curr Opin Microbiol 10(3):246–253.

Miller JH. 1992. A short course in bacterial genetics. Cold Spring Harbor Laboratory Press.

Morrison BA, Shain DH. 2008. An AMP nucleosidase gene knockout in *Escherichia coli* elevates intracellular ATP levels and increases cold tolerance. Biol Lett 4(1):53–56.

Murakami K, Tsubouchi R, Fukayama M, Ogawa T, Yoshino M. 2006. Oxidative inactivation of reduced NADP-generating enzymes in *E. coli*: Iron-dependent inactivation with affinity cleavage of NADP-isocitrate dehydrogenase. Arch Microbiol 186(5):385–392.

Mureev S, Kovtun O, Nguyen UTT, Alexandrov K. 2009. Species-independent translational leaders facilitate cell-free expression. Nat Biotechnol 27(8):747–752.

Nahalka J, Chen ZLX, Wang PG. 2003. Superbeads: Immobilization in ''sweet'' chemistry. Chem Eur J 9(2):372–377.

Sambrook J, Russel, DW 2001. Molecular cloning: A laboratory manual. 3rd edn.: Cold Spring Harbor, New York, Cold Spring Harbor Laboratory Press.

Sauer U, Canonaco F, Heri S, Perrenoud A, Fischer E. 2004. The soluble and membrane-bound transhydrogenases UdhA and PntAB have divergent functions in NADPH metabolism of *Escherichia coli*. J Biol Chem 279(8):6613–6619.

Scamuffa MD, Caprioli RM. 1980. Comparison of the mechanisms of two distinct aldolases from *Escherichia coli* grown on gluconeogenic substrates. Biochim Biophys Acta 614(2):583–590.

Schoevaart R, van Rantwijk F, Sheldon RA. 1999. Class I fructose-1,6-bisphosphate aldolases as catalysts for asymmetric aldol reactions. Tetrahedron: Asymmetry 10(4):705–711.

Schümperli M, Pellaux R, Panke S. 2007. Chemical and enzymatic routes to dihydroxyacetone phosphate. Appl Microbiol Biotechnol 75(1):33–45.

Sheflyan GY, Howe DL, Wilson TL, Woodard RW. 1998. Enzymatic synthesis of 3-deoxy-D-manno-octulosonate 8-phosphate, 3-deoxy-D-altro-octulosonate 8-phosphate, 3,5-dideoxy-D-gluco(manno)-octulosonate 8-phosphate by 3-deoxy-D-arabino-heptulosonate 7-phosphate synthase. J Am Chem Soc 120(43):11027–11032.

Shimizu Y, Inoue A, Tomari Y, Suzuki T, Yokogawa T, Nishikawa K, Ueda T. 2001. Cell-free translation reconstituted with purified components. Nat Biotechnol 19(8):751–755.

Swartz J. 2006. Developing cell-free biology for industrial applications. J Ind Microbiol Biotechnol 33(7):476–485.

Valsesia G, Medaglia G, Held M, Minas W, Panke S. 2007. Circumventing the effect of product toxicity: Development of a novel two-stage production process for the lantibiotic gallidermin. Appl Environ Microbiol 73(5):1635–1645.

Welch P, Scopes RK. 1985. Studies on cell-free metabolism: Ethanol production by a yeast glycolytic system reconstituted from purified enzymes. J Biotechnol 2(5):257–273.

Wong CH, Whitesides GM. 1983. Synthesis of sugars by aldolase-catalyzed condensation reactions. J Org Chem 48(19):3199–3205.

Zelic B, Gerharz T, Bott M, Vasic-Racki D, Wandrey C, Takors R. 2003. Fed-batch process for pyruvate production by recombinant *Escherichia coli* YYC202 strain. Eng Life Sci 3(7):299–305.

Zhang YHP, Evans BR, Mielenz JR, Hopkins RC, Adams MWW. 2007. High-yield hydrogen production from starch and water by a synthetic enzymatic pathway. PLoS ONE 2(5):e456.